RSC Advances

PAPER

Cite this: *RSC Adv.*, 2018, **8**, 38831

A novel electrolyte additive for improving the interfacial stability of $LiMn_2O_4$ cathode lithium-ion batteries at elevated temperature†

T. Huang, X. Zheng, G. Fang, Y. Pan, W. Wang and M. Wu *

Received 9th October 2018
Accepted 5th November 2018

DOI: 10.1039/c8ra08355j

rsc.li/rsc-advances

Methanesulfonic acid 2,2,3,3-tetrafluoropropyl (TFPMS) is newly explored as a protection additive to improve the interfacial stability of $LiMn_2O_4$ cathode/electrolyte at an elevated temperature. At 1C rate, the addition of 0.5 vol% TFPMS improves the capacity retention of an $LiMn_2O_4$/Li cell from 56.9% to 72.9% after 200 cycles at 55 °C. Electrochemical impedance spectroscopy (EIS) and transmission electron microscopy (TEM) results suggest that the electrolyte with 0.5 vol% TFPMS forms a thinner and less resistive interface. X-ray photoelectron spectroscopy (XPS) analysis reveals that the addition of TFPMS restrains the formation of LiF and Li_2CO_3. Moreover, X-ray diffraction (XRD) and inductively coupled plasma (ICP) analysis confirms the effectiveness of TFPMS-enhanced structural stability of $LiMn_2O_4$.

Introduction

$LiMn_2O_4$ is an ideal high-power cathode material for lithium-ion batteries because of its high thermal stability, low manufacturing cost, environmentally friendly nature, high energy density and long life cycles. However, capacity fading of $LiMn_2O_4$-based batteries at high temperatures is still a barrier for practical applications. The reasons for capacity fading and poor thermostability are the following possible mechanisms[1–5]: (1) $LiPF_6$-based carbonate electrolyte decomposition, (2) manganese dissolution: $2Mn^{3+}$ (s) = Mn^{2+} (aq.) + Mn^{4+} (s) on the surface of the $LiMn_2O_4$ electrode, (3) irreversible crystal phase transition (Jahn–Teller distortion), and (4) oxygen deficiency.

Methods such as element doping[6–9] and surface coating[10–12] have been proposed in previous studies. The electrolyte is one of the main factors for serious deterioration of $LiMn_2O_4$-based batteries at elevated temperatures. Recently, researchers have used new lithium salts and functional electrolyte additives to improve cyclic stability.

It is reported that lithium difluoro(oxalato)borate, instead of $LiPF_6$, can improve the capacity retention of an $LiMn_2O_4$ cathode significantly after 100 cycles at 25 °C and 60 °C.[13] X. J. Huang *et al.* reported that LiFNFSI as a single electrolyte salt improves the stability of $LiMn_2O_4$ at 60 °C.[14] Some new lithium salts, such as LiTFSI, LiFAP, and LiBETI, with properties superior to those of $LiPF_6$ have been evaluated.[15,16] However, the new lithium salts due to some of their own drawbacks have not fully replaced $LiPF_6$ in $LiMn_2O_4$-based batteries in recent years.

Using a functional additive is the most economical and effective method. W. T. Li *et al.* mentioned that the addition of 3% DMAc to an electrolyte increases the thermal stability of the electrolyte and reduces both surface corrosion and deposition of electrolyte decomposition products on $LiMn_2O_4$ particles.[17] Y. K. Li *et al.* reported that the stability of batteries using electrolytes with 0.1 wt% heptamethyldisilazane can be improved after storage at 60 °C for 7 days.[18] L. Li *et al.* used tris (trimethylsilyl) borate (TMSB) as an effective SEI electrolyte additive to improve the cycling performance of an $LiMn_2O_4$ lithium-ion battery at both room temperature and 55 °C.[19] Park *et al.* added 2 wt% fluoroethylene carbonate (FEC) into an electrolyte (EC/DEC/PC with 1 M $LiPF_6$). When 2 wt% FEC was added, the capacity retention at 60 °C after 130 cycles significantly improved by about 20%.[20] W. Li *et al.* reported that trimethyl borate (TPB) can stabilize the $LiMn_2O_4$/carbonate-based electrolyte interface.[21] Nan *et al.* evaluated the effectiveness of 0.5 wt% MMDS in $LiMn_2O_4$-based LIBs on the cycling performance at 60 °C and capacity retention storage at 85 °C.[22]

In this study, methanesulfonic acid 2,2,3,3-tetrafluoropropyl (TFPMS) was synthesized and used as a new SEI-forming additive for lithium-ion batteries. It was found to be effective for stabilizing the interface between $LiMn_2O_4$ and a carbonate-based electrolyte at 55 °C. The effect of TFPMS was investigated using electrochemical impedance spectroscopy (EIS), X-ray photoelectron spectroscopy (XPS), transmission electron microscopy (TEM), nuclear magnetic resonance spectroscopy (NMR), X-ray diffraction (XRD) and inductively coupled plasma (ICP).

Key Laboratory of Optoelectronic Materials Chemistry and Physics, Fujian Institute of Research on the Structure of Matter, Chinese Academy of Sciences, Fuzhou 350002, P. R. China. E-mail: mxwu@fjirsm.ac.cn

† Electronic supplementary information (ESI) available. See DOI: 10.1039/c8ra08355j

Experimental

Preparation of electrolyte

TFPMS was synthesized in our laboratory. 2,2,3,3-Tetrafluoro-1-propanol (176 g, 1.33 mol) and triethylamine (157 g, 1.56 mol) were added to a round flask, stirred and cooled to 10 °C in an ice bath. Then, under stirring, methylanesulfonyl chloride (145 g, 1.26 mol) was added dropwise from a dropping funnel with the reaction mixture temperature controlled below 10 °C. Next, the mixture was stirred at 50 °C for another 6 h. Then, the mixture was cooled to room temperature and deionized water (300 ml) was added. The organic layer was washed with deionized water 6 times and dried over anhydrous magnesium sulphate. Methanesulfonic acid 2,2,3,3-tetrafluoropropyl ester was obtained by fractional distillation under vacuum with 185 g (70%) yield.

^{1}H-NMR ($CDCl_3$, ppm): 5.95 (tri, 1H); 4.55 (tri, 2H); 3.12 (s, 3H).^{13}C-NMR ($CDCl_3$, ppm): 115.87 (tri); 113.38 (tri); 111.47 (tri); 110.88 (tri); 108.99 (tri); 106.50 (tri); 63.65 (tri); 37.84.

Electrolytes of 1 M $LiPF_6$/EC + DMC + EMC (Dongguan Shanshan Battery Materials Co., Ltd.) with and without 0.5 vol% TFPMS were prepared in an argon atmosphere glove box (the oxygen and water contents were less than 5 ppm).

Cell assembly

The $LiMn_2O_4$ electrode with an active mass loading of about 2.3 mg cm^{-2} was prepared by combining 80 wt% $LiMn_2O_4$, 10 wt% polyvinylidene fluoride (PVDF) and 10 wt% acetylene black. Also, 2025-type coin cells were assembled in an argon atmosphere glove box using a lithium sheet as the anode, the above $LiMn_2O_4$ electrode as the cathode, 1 M $LiPF_6$/EC + DMC + EMC with and without 0.5 vol% TFPMS as electrolytes (ESI 1†), and Celgard 2325 porous polypropylene as a separator.

Electrochemical measurements

Cycling performance testing of $LiMn_2O_4$/Li cells was carried out on a Land cell tester, CT2001A. The formation cycles were as follows: 0.1C (1C = 148 mA g^{-1}) three times, 0.2C three times, 0.5C three times, and 1.0C three times at 25 °C under constant current conditions from 3.0 to 4.3 V. The $LiMn_2O_4$/Li cells were then cycled at 1.0C at 55 °C for the cycling performance test. The $LiMn_2O_4$/Li cells were then cycled at 0.1C, 0.2C, 0.5C, 1C, and 5C at 25 °C for rate performances. The EIS measurements were tested through a frequency response analyzer (VSP, Bio-logic). EIS measurements were tested at the fully delithiated state of 4.3 V for $LiMn_2O_4$/Li cells. The frequency range was from 100 kHz to 10 MHz, and the amplitude was 5 mV.

Physical characterizations

The cycled $LiMn_2O_4$ was disassembled in a glove box and washed three times with DMC solvent to remove the residual electrolyte. TEM measurements were performed with JEM-2010, JEOL. The XPS measurements were obtained with an X-ray photoelectron spectrometer (ESCALAB 250, USA) to investigate the interfacial components of the electrodes. The electrolyte was taken from the cells, which were disassembled in an argon atmosphere glove box. ^{1}H NMR data of the electrolytes were tested by NMR (AVANCE III, Bruker Biospin) using a CD_3CN solvent. The crystal structure was identified by X-ray diffraction (XRD, Bruker D8 ADVANCE) using Cu Kα radiation. ICP analysis was carried out on IRIS Intrepid II XSP. The cycled lithium electrodes for ICP analyses were rinsed with DMC solvent three times and dissolved in 5.0 wt% HNO_3.

Results and discussion

Fig. 1 presents the cyclic stability of $LiMn_2O_4$ electrodes in electrolytes without and with 0.5 vol% TFPMS at 1.0C at 55 °C after 200 cycles. The discharge capacity of $LiMn_2O_4$ without an additive at the first cycle was 105 mA h g^{-1} but became 59.7 mA h g^{-1} after 200 cycles. After adding 0.5 vol% TFPMS into the electrolyte, the cyclic stability of $LiMn_2O_4$ improved, becoming 76.6 mA h g^{-1}. The coulombic efficiencies of 0.5 vol% TFPMS-containing Li/$LiMn_2O_4$ cells were better than that of the cell with no additive. Apparently, TFPMS could provide protection for $LiMn_2O_4$ at an elevated temperature. The charge–discharge profiles of the $LiMn_2O_4$/Li cells cycled at 55 °C are shown in ESI 2.† The change in the charge–discharge platform of the cell without an additive was larger than that observed for the cell containing TFPMS additive. Unlike the cell with the electrolyte without additive, the cell with the electrolyte containing 0.5 vol% TFPMS additive exhibited negligible polarization and smooth charge–discharge profiles.

The discharge curves and corresponding differential capacity (dQ/dV) plots of $LiMn_2O_4$/Li cells cycled in electrolyte with and without TFPMS after different cycles are shown in Fig. 2. From Fig. 2(a) and (c), we can see that the discharge capacity and voltage plateau of the electrode in the electrolyte without the additive fade quickly compared with those of the electrode in the electrolyte with 0.5 vol% TFPMS after 200 cycles, indicating that the latter exhibits smaller electrochemical polarization. Differential capacity plots exhibit two main peaks located at around 3.98 V and 4.1 V at the 1st cycle, as shown in Fig. 2(b) and (d). All these peaks shift negatively with cycling in the electrolyte with and without the additive. This shows that the

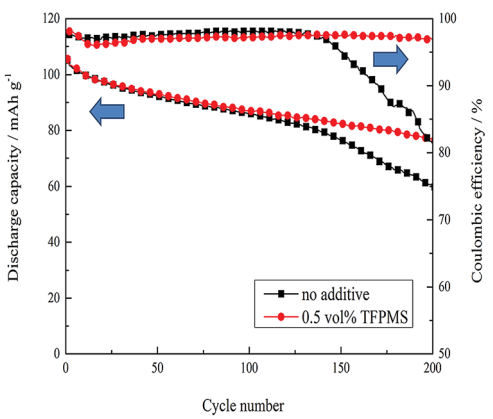

Fig. 1 The cyclic stability of $LiMn_2O_4$ electrodes in the electrolytes without and with 0.5 vol% TFPMS at 1.0C at 55 °C after 200 cycles.

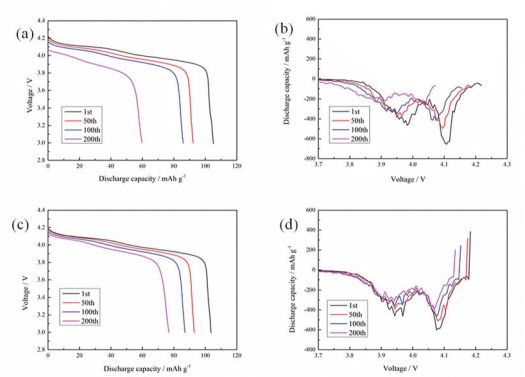

Fig. 2 Selected discharge curves and corresponding dQ/dV plots of $LiMn_2O_4$ electrode in the electrolytes without (a and b) and with 0.5 vol% TFPMS (c and d).

peak position shift becomes less significant in the TFPMS-containing electrolyte compared to that for the electrolyte without the additive after cycling, which can be ascribed to the protection provided by the cathode interface film due to TFPMS.

The rate capability of the cathode is influenced by polarization. A rate performance study is carried out, as shown in Fig. 3. It can be seen that the cell with 0.5 vol% TFPMS displays better rate performance than that without the additive (especially at 5C), suggesting that the incorporation of TFPMS can decrease polarization.

EIS measurements were obtained at the fully delithiated state of 4.3 V for $LiMn_2O_4$/Li cells. The EIS spectra of the cells mainly include bulk resistance (R_e), SEI resistance (R_f), and charge transfer resistance (R_{ct}). Fig. 4 presents the EIS of $LiMn_2O_4$/Li cells with different electrolytes. Re is the bulk resistance of the cell, which reflects the electric conductivity of the electrolyte, separator, and electrodes. Also, 0.5 vol% concentration of TFPMS in the electrolyte was shown to have a negligible effect on the electrical conductivity of the electrolytes. Thus, the values of R_e with different electrolytes are nearly the same. After the formation cycle at 25 °C, it can be found that R_f and R_{ct} with different electrolytes are nearly the same. However, after 200 cycles at 55 °C, R_f of the cell with TFPMS

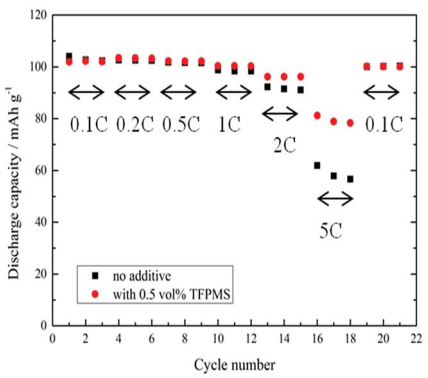

Fig. 3 The rate performances of $LiMn_2O_4$/Li cells cycled in the electrolytes with and without TFPMS at different charge/discharge rates.

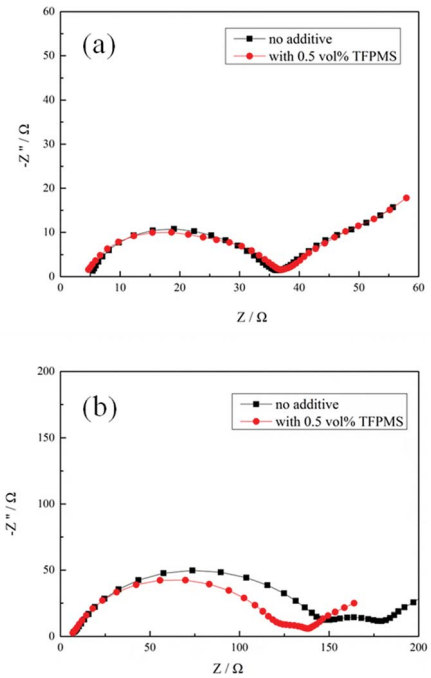

Fig. 4 EIS of $LiMn_2O_4$/Li cells with and without 0.5 vol% TFPMS after (a) formation at 25 °C and (b) 200 cycles at 55 °C.

(59.53 Ω) is smaller than that of the cell without the additive (63.51 Ω), and the lower R_f value implies that SEI due to TFPMS can be thinner. R_{ct} of the cell with TFPMS (81.31 Ω) is significantly smaller than that of the cell without the additive (116.6 Ω), showing that the charge transfer is easier through the film; this confirms the ability of TFPMS in hindering the increase in electrode polarization. This is in agreement with the results shown in Fig. 2.

Fig. 5 shows ^{1}H NMR data of the electrolytes with 0.5 vol% TFPMS before and after formation at 25 °C and 200 cycles at 55 °C. The peaks at 5.9–6.2 ppm were assigned to –CF_2H of TFPMS, and the peak appearing at 3.17 ppm corresponded to –CH_3 of TFPMS. The TFPMS peaks disappeared after 200 cycles. Based on EIS and NMR results, we believe that SEI on the $LiMn_2O_4$ surface is formed gradually during cycling due to TFPMS.

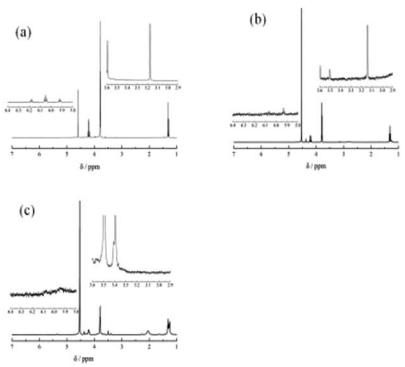

Fig. 5 ^{1}H NMR data of the electrolytes with 0.5 vol% TFPMS before (a) and after formation at 25 °C (b) and 200 cycles at 55 °C (c).

TEM images (Fig. 6) show the edges of $LiMn_2O_4$ particles after being cycled with different electrolytes at 55 °C. After cycling, in the electrolyte without the additive, the $LiMn_2O_4$ particles are covered with a thick deposit, as shown in Fig. 6(a). The TEM image in Fig. 6(b) shows that a thin and uniform film exists on $LiMn_2O_4$ particles, indicating that a protective SEI film has been formed due to TFPMS.

Fig. 7 presents the XPS spectra of the observed elements on the $LiMn_2O_4$ electrode cycled in different electrolytes at 55 °C. In the Mn 2p spectra, three main peaks can be found. The peaks located at 641.7 eV, 642.9 eV, and 653.6 eV correspond to Mn^{3+}, Mn^{4+}, and Mn $2p^{1/2}$.[23] The O 1s spectrum is dominated by the peak of O–Mn (529.6 eV[24]) in metal oxide, C=O (531.3 eV[25,26]), C–O (533.3 eV[25,26]), and Li_2CO_3 (532 eV[25]). There are two characteristic peaks in the F 1s spectra: LiF (684.5eV[27]) and PVDF (687.6 eV[28]). The Mn peaks of Mn 2p and Mn–O of O 1s for the electrode with TFPMS are stronger than that for the electrode without the additive, confirming that the CEI film from electrolyte decomposition is thinner due to TFPMS. When 0.5 vol% TFPMS is added, the intensity of the C=O peak of O 1s decreases, whereas the intensity of the C–O peak of O 1s increases, suggesting that TFPMS can efficiently hinder the polymerization of EC solvent. The intensities of Li_2CO_3 of O 1s and LiF of F 1s on the $LiMn_2O_4$ electrode with TFPMS are much smaller than those without the additive, suggesting that the $LiMn_2O_4$ cathode electrode with TFPMS is covered with less inorganic degradation products. This leads to decreased R_f and R_{ct} of the cells with 0.5 vol% TFPMS. The C 1s peaks located at 290.3 eV and 285.7 eV correspond to the PVDF binder.[22] The peaks at 284.7 eV,[29] 288.5 eV,[29] and 286.5 eV[30] are assigned to graphite, C=O and C–O, respectively. There are only minor differences seen, which is in accordance with the O 2p spectra. However, there is a small peak at 292.7 eV[31] from C–F, which indicates the existence of C–F due to the decomposition of TFPMS on the cathode surface film. This is because C–F is the functional group of the TFPMS additive. The existence of S indicates that TFPMS contributes to the surface film of the cathode. The S 2p spectrum at 169 eV in our analysis can be assigned to $ROSO_2Li$.[32,33] The possible reaction paths of TFPMS are presented in Fig. 8.[34]

Fig. 9 presents the XRD spectra of $LiMn_2O_4$ electrodes cycled in different electrolytes at 55 °C. The intensities of all the $LiMn_2O_4$ diffraction peaks of the electrodes become weaker compared to that of the pristine electrode, which may be due to the dissolution of Mn^{2+} in the electrolyte at an elevated temperature.[19,35,36] It can be found that the peak intensities of the electrodes with TFPMS are stronger than those of the electrode without the additive. The diffraction peaks (111) of the cycled cathodes shift to higher angles, whereas the extent of the shift in the peaks of the electrode without the additive is much larger than that with the additive. This indicates that the extent of degradation of the spinel structure of $LiMn_2O_4$ in the electrode with TFPMS is much weaker than that without the additive, which is in accordance with the Mn 2p spectra as discussed above.

Manganese metal dissolved from $LiMn_2O_4$ is also deposited on the anode, which can be confirmed by analyzing the

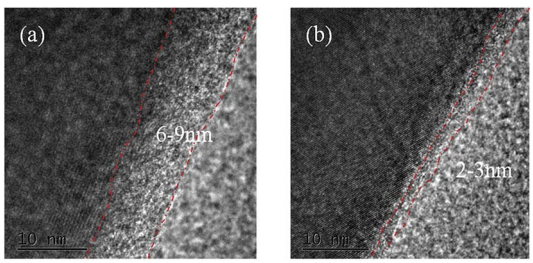

Fig. 6 TEM images of $LiMn_2O_4$ cathodes after 200 cycles at 55 °C in the electrolyte (a) without and (b) with 0.5 vol% TFPMS.

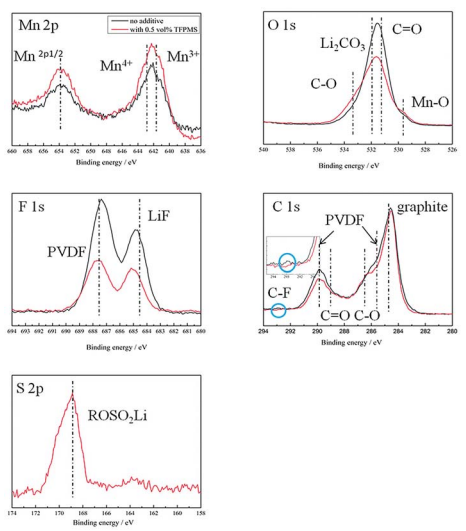

Fig. 7 The XPS spectra of $LiMn_2O_4$ cathodes cycled in different electrolytes at 55 °C.

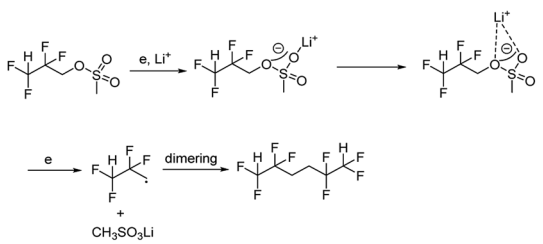

Fig. 8 The possible reaction paths of TFPMS on the cathode.

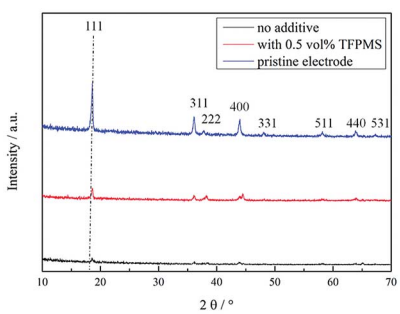

Fig. 9 The XRD spectra of $LiMn_2O_4$ cathodes cycled in different electrolytes at 55 °C.

elemental contents on the lithium electrode. The contents of Mn are 1.46 ppm for the electrolyte without the additive and 1.05 ppm for the electrolyte with TFPMS. The contents of Mn on the lithium electrode cycled in the electrolyte without TFPMS are higher than those in the electrolyte with 0.5 vol% TFPMS. TFPMS shows better ability to suppress manganese metal dissolution, resulting in enhanced structural stability of $LiMn_2O_4$.

Conclusions

In summary, TFPMS can be used as an effective electrolyte additive for the formation of a stable SEI layer on the $LiMn_2O_4$ electrode at 55 °C. The addition of 0.5 vol% TFPMS can increase the cycling and rate performance of $LiMn_2O_4$/Li cells. After 200 cycles at 55 °C, the capacity retention is significantly increased from 56.9% to 72.9% with TFPMS. The stable SEI layer derived from TFPMS is thinner and less resistive, and we also observe enhanced structural stability of $LiMn_2O_4$.

Conflicts of interest

There are no conflicts to declare.

Acknowledgements

This work was supported by the National Key Research and Development Program of China (Grant No. 2016YFB0100100), the National Natural Science Foundation of China (Grant No. 21805279) and the Science and Technology Planning Project of Fujian Province (Grant No. 2017H0045, 2016T3012).

Notes and references

1 K. Y. Chung, H. S. Lee, W. S. Yoon, J. McBreen and X. Q. Yang, *J. Electrochem. Soc.*, 2006, **153**, A774–A780.
2 J. Cho and M. M. Thackeray, *J. Electrochem. Soc.*, 1999, **146**, 3577–3581.
3 C. L. Campion, W. T. Li and B. L. Lucht, *J. Electrochem. Soc.*, 2005, **152**, A2327–A2334.
4 M. W-Mehrens, C. Vogler and J. Garche, *J. Power Sources*, 2004, **127**, 58–64.
5 L. Yang, M. Takahashi and B. F. Wang, *Electrochim. Acta*, 2006, **51**, 3228–3234.
6 L. L. Xiong, Y. L. Xu, T. Tao and J. B. Goodenough, *J. Power Sources*, 2012, **199**, 214–219.
7 M. Prabu, M. V. Reddy, S. Selvasekarapandian, G. V. Subba Rao and B. V. R. Chowdari, *Electrochim. Acta*, 2013, **88**, 745–755.
8 Z. D. Peng, Q. L. Jiang, K. Du, W. G. Wang, G. R. Hu and Y. X. Liu, *J. Alloys Compd.*, 2010, **493**, 640–644.
9 M. V. Reddy, A. Sakunthala, S. SelvasekaraPandian and B. V. R. Chowdari, *J. Phys. Chem. C*, 2013, **117**, 9056–9064.
10 D. H. Hu, S. X. Zhao, Y. F. Deng and C. W. Nan, *J. Mater. Chem. A*, 2013, **1**, 14729–14735.
11 X. Q. Wang, O. Tanaike, M. Kodama and H. Hatori, *J. Power Sources*, 2007, **168**, 282–287.
12 S. Zhao, Y. Bai, Q. J. Chang, Y. Q. Yang and W. F. Zhang, *Electrochim. Acta*, 2013, **108**, 727–735.
13 M. H. Fua, K. L. Huang, S. Q. Liu, J. S. Liu and Y. K. Li, *J. Power Sources*, 2010, **195**, 862–866.
14 S. Zhou, H. Han, J. Nie, M. Armand, Z. Zhou and X. Huang, *J. Electrochem. Soc.*, 2012, **159**, A1158–A1164.
15 P. X. Han, B. Zhang, C. S. Huang, L. Gu, H. Li and G. L. Cui, *Electrochem. Commun.*, 2014, **44**, 70–73.
16 J. S. Gnanaraj, E. Zinigrad, M. D. Levi, D. Aurbach and M. Schmidt, *J. Power Sources*, 2003, **119–121**, 799–804.
17 W. Li and B. L. Lucht, Inhibition of solid electrolyte interface formation on cathode particles for lithium-ion batteries, *J. Power Sources*, 2007, **168**, 258–264.
18 Y. Li, R. Zhang, J. Liu and C. Yang, *J. Power Sources*, 2009, **189**, 685–688.
19 Y. Liu, L. Tan and L. Li, *J. Power Sources*, 2013, **221**, 90–96.
20 M. H. Ryou, G. B. Han, Y. M. Lee, J. N. Lee, D. J. Lee, Y. O. Yoon and J. K. Park, *Electrochim. Acta*, 2010, **55**, 2073–2077.
21 X. Yang, J. Li, L. Xing, Y. Liao, M. Xu, Q. Huang and W. Li, *Electrochim. Acta*, 2017, **227**, 24–32.
22 X. Zuo, J. Wu, C. Fan, K. Lai, J. Liu and J. Nan, *Electrochim. Acta*, 2014, **130**, 778–784.
23 N. Treuil, C. Labrugere, M. Menetrier, J. Portier, G. Gampet, A. Deshayes, J. C. Frison, S. J. Hwang, S. W. Song and J. H. Choy, *J. Phys. Chem. B*, 1999, **103**, 2100–2106.
24 X. Zuo, C. Fan, X. Xiao, J. Liu and J. Nan, *J. Power Sources*, 2012, **219**, 94–99.
25 K. A. Striebel, E. Sakai and E. J. Cairns, *J. Electrochem. Soc.*, 2002, **149**, A61–A68.
26 L. Yang, B. Ravdel and B. L. Lucht, *Electrochem. Solid-State Lett.*, 2010, **13**, A95–A97.
27 D. Chalasani, J. Li, N. M. Jackson, M. Payne and B. L. Lucht, *J. Power Sources*, 2012, **208**, 67–73.
28 B. Li, M. Q. Xu, B. Z. Li, Y. L. Liu, L. Yang, W. S. Li and S. J. Hu, Properties of solid electrolyte interphase formed by prop-1-ene-1,3-sultone on graphite anode of Li-ion batteries, *Electrochim. Acta*, 2013, **105**, 1–6.
29 L. Yang, T. Markmaitree and B. L. Lucht, *J. Power Sources*, 2011, **196**, 2251–2254.
30 H. Rong, M. Xu, L. Xing and W. Li, *J. Power Sources*, 2014, **261**, 148–155.
31 G. Nans'e, E. Papirer, P. Fioux, F. Moguet and A. Tressaud, *Carbon*, 1997, **35**, 175–194.
32 H. Ota, T. Akai, H. Namita, S. Yamaguchi and M. Nomura, *J. Power Sources*, 2003, **119–121**, 567–571.
33 A. Sano and S. Maruyama, *J. Power Sources*, 2009, **192**, 714–718.
34 T. Huang, M. Wu, W. Wang, Y. Pan and G. Fang, *J. Power Sources*, 2014, **262**, 303–309.
35 C. J. Curtis, J. Wang and D. L. Schulz, *J. Electrochem. Soc.*, 2004, **151**, A590–A598.
36 J. B. Goodenough, *J. Power Sources*, 2007, **174**, 996–1000.